High-Internal-Phase Emulsion Tailoring Polymer Amphiphilicity towards an Efficient NIR-Sensitive Bacteria Filter

*Xiaopeng Huang, Youdi Yang, Jiezhong Shi, Huynh Thien Ngo, Chaohua Shen, Wenbin Du, and Yapei Wang**

Emulsions having a high internal-phase volume fraction—termed as HIPEs for high internal phase emulsions—are in high demand as templates for functional macroporous materials. Designing molecular surfactants with appropriate amphiphilicity plays a critical role in the HIPE preparation. In this study, successful tailoring of the amphiphilicity of the originally hydrophobic block co-polymer of polystyrene-b-polyvinylpyridine (PS-b-P4VP) is reported. In combination with trifluoroacetic acid, less than 5 wt% of the polymer–CF_3COOH system is feasible as a surfactant for HIPE preparation; this is lower than the amounts typically needed for commonly used commercial surfactants. Using the HIPEs as templates, well-defined closed- and open-cell macroporous triacrylate-based monoliths are fabricated simply through the adjustment of the ratio of the water phase to oil phase. After coating the resulting macroporous material with polypyrrole nanoparticles, the system can be exploited as an NIR-sensitive filter for bacteria; it not only excludes oversized bacteria, but it also kills the bacteria with the help of NIR-induced heat.

1. Introduction

Characterized by the internal-phase volume fraction exceeding 74%, high-internal-phase emulsions (HIPEs) have attracted tremendous attention during the last few decades due to their extensive applications in the food, cosmetic, coating, and petrochemical industries.[1] They also provide a facile, versatile, and large-scale platform for the preparation of macroporous materials, broadening the range of their applications to the fields of cell culture, catalyst support, energy storage, and environmental protection.[2] The preparation of macroporous materials can be achieved by polymerizing the concentrated continuous phase followed by removing the dispersion phase, resulting in a macroporous polymeric scaffold known as PolyHIPE. In contrast to hard templates such as inorganic and organic colloids,[3] HIPEs possess noticeable simplicity and flexibility. They also exhibit superior controllability and long-term stability compared to some other soft templates such as supercritical fluid and bubbled gas.[4] In this respect, exploring advanced techniques towards HIPEs is of significant importance for the development of functional macroporous materials.

In general, common emulsions will undergo unstable behaviors, e.g., phase inversion and phase separation (or "creaming"), when the internal-phase volume is excessive; however, in a typical HIPE system, droplets either take the form of broad polydispersity or deform to polyhedra, thus attaining an extraordinarily high internal-phase volume over

X. Huang, Y. Yang, J. Shi, Prof. Y. Wang
Department of Chemistry
Renmin University of China
Beijing 100872, China
E-mail: yapeiwang@ruc.edu.cn
Dr. H. T. Ngo
National Institute for Materials Science (NIMS-MANA)
Namiki 1–1, Tsukuba, Ibaraki 305–0044, Japan
C. Shen, Prof. W. Du
State Key Laboratory of Microbial Resources
Institute of Microbiology
Chinese Academy of Sciences
Beijing 100101, China

DOI: 10.1002/smll.201501396

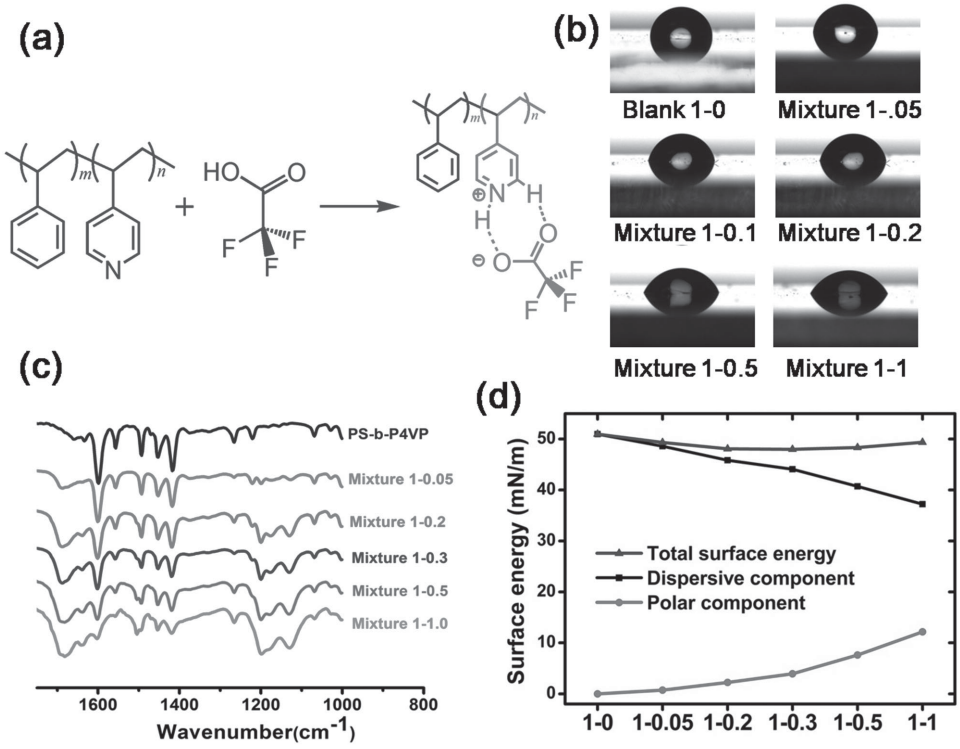

Figure 1. a) Schematic of the quaternization reaction between the PS-*b*-P4VP and CF_3COOH. b) Contact angles, c) FT-IR spectra, and d) surface energies of different mixtures consisting of PS-*b*-P4VP and CF_3COOH, where the molar ratio of pyridine rings to carboxyl groups varies from 1:0 (denoted as "Mixture 1–0") to 1:1 (denoted as "Mixture 1–1").

the closest-packed volume of 74%.[1b,c] This property benefits from the surfactants or interfacially active particles which are capable of firmly absorbing at the water-in-oil (W/O) interface, establishing the mechanical barrier and avoiding droplet coalescence and phase inversion. Commercially available small-molecule surfactants—such as sodium dodecyl sulfate (SDS), cetyltrimethylammonium bromide (CTAB), and Span 80—either individually or jointly used, are the primary choices. However, because of the intrinsically dynamic stabilization, a significant amount of surfactant (at least 5 wt%, typically 20 wt%) is required for the HIPE preparation.[5] Sub-micrometer solid particles are employed as alternative stabilizers due to their irreversible "anchor" at the W/O interface, where the emulsions are known as Pickering emulsions. Nevertheless, the interfacial activity of the particles is relatively insufficient, and for a long time, the maximum internal-phase volume has been theoretically and experimentally deemed as 70%, above which phase inversion occurs.[6] Recently , real Pickering HIPEs with an internal-phase volume of above 80% were prepared via deliberate surface modification of the particles. The particle geometry and dimension should also be well regulated in order to avoid the instability caused by gravity and Brownian motion. In addition, the polymerization of Pickering HIPEs usually resulted in a closed-cell macroporous structure, which may limit their applications in many fields such as separation, catalysis, and tissue engineering.[7]

Polymers are another type of common-used surfactants. They offer significant advantages over small molecules and solid particles in terms of interfacial stabilization and biocompatibility. Owing to their characteristic amphiphilic structure and effective steric arrangement, they have great potential for use in HIPE preparation. Traditionally, the polymeric surfactants suitable for HIPE preparation have been limited to several kinds of polyethylene oxide (PEO)-based co-polymers, such as Pluronic and Hypermer.[8] Recently, more and more efforts have been directed at the design of amphiphilic block co-polymers that can be used for the stabilization of HIPEs, which can provide a one-step route for the surface functionalization of the 3D matrix.[9] Despite the considerable importance of the polymeric amphiphilicity for HIPE preparation, a systematic rule for the selection of the block co-polymer with an appropriate amphiphilicity is unknown to our knowledge. As part of an ongoing study for tailoring polymeric amphiphilicity towards controllable emulsions,[10] herein, we disclose a new protocol for the preparation of W/O HIPEs with an internal-phase volume of up to 95%, solely using an amphiphilicity-adjustable diblock co-polymer in small amounts. A facile and rapid route for tailoring the polymer amphiphilicity was exploited, enabling systematic investigation of the influence of polymer amphiphilicity on the phase behaviors of emulsions. Functional macroporous architectures templated from the HIPE were fabricated for further applications.

2. Results and Discussion

2.1. Tailoring the Amphiphilicity of Block Co-polymers

As shown in **Figure 1**a, the amphiphilicity-adjustable block co-polymer used for emulsification was

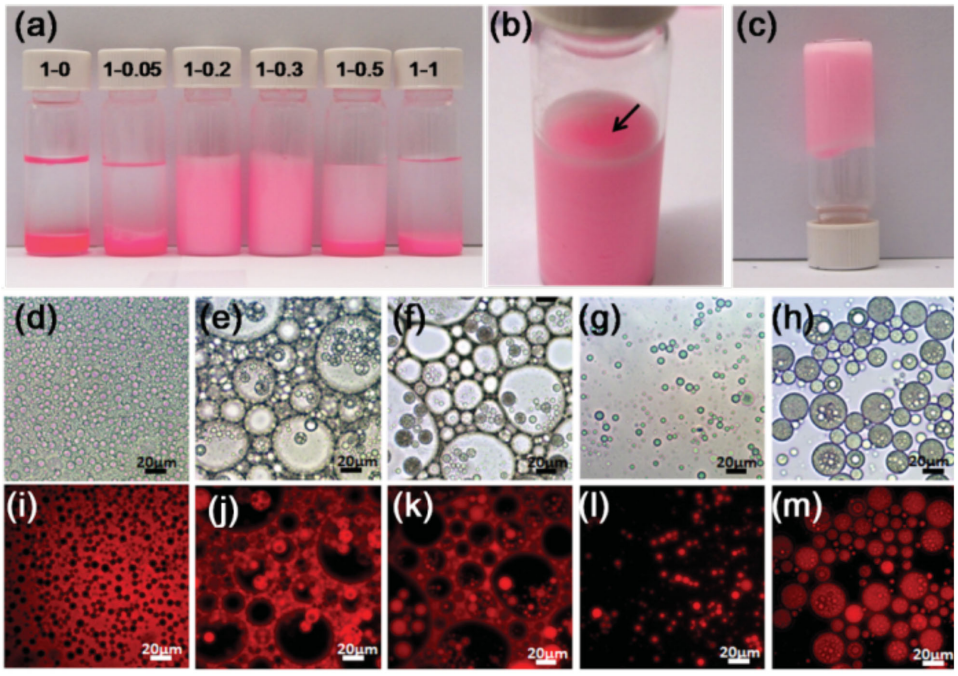

Figure 2. a) Optical, d–h) bright-field microscopy , and i–m) fluorescence images of the emulsions prepared using different mixtures of PS-*b*-P4VP and CF_3COOH, where the molar ratio of pyridine rings to carboxyl groups is denoted: 1:0, 1:0.05 (Emulsion 1-0.05, d,i), 1:0.2 (Emulsion 1-0.2, e,j), 1:0.3 (Emulsion 1-0.3, f,k), 1:0.5 (Emulsion 1-0.5, g,l), and 1:1 (Emulsion1-1, h,m). b,c) Close-up optical images of the Emulsion 1–0.2 immediately after vortex emulsification (b) and after being stored upside down for two weeks (c). The arrow in (b) indicates the evident concave surface above the emulsion.

polystyrene-*b*-polyvinylpyridine (PS-*b*-P4VP; M_n = 8800 Da; PDI = 1.15). Generally, this block co-polymer is hydrophobic, indicated by a water contact angle of 95° (Figure 1b and Table S1 in the Supporting Information, SI). The quaternization reaction with the small molecule, trifluoroacetic acid (CF_3COOH), results in the hydrophilization of the P4VP segment, therefore forming the amphiphilic structure. A gradual decrease in the water contact angle is shown in Figure 1b; with an increasing amount of CF_3COOH, the contact angle approaches 60° for Mixture 1–1 (denoted the mixture with a molar ratio of 1:1 of the pyridine rings to carboxyl groups). Amphiphilic enhancement can be also reflected by surface energies. The polar components, which are connected with the affinity to water, present an obvious growth (Figure 1d; Table S1, SI). Fourier-transform IR (FTIR) spectroscopy is then used to characterize the growing quaternization degree of the amphiphilic mixtures (Figure 1c). Originally the characteristic peaks associated with pyridine rings, 1598 and 1415 cm^{-1}, shift to 1602 and 1419 cm^{-1}, respectively, and new characteristic peaks form at 1637 and 1675 cm^{-1} due to the N–H interaction and carboxyl groups, respectively. It is worth mentioning that this method for tailoring the amphiphilicity of PS-*b*-P4VP is rather facile and controllable, which is achieved by mixing PS-*b*-P4VP with desired amounts of CF_3COOH in dichloromethane (DCM).

2.2. High Internal Phase Emulsions (HIPEs)

To demonstrate the interfacial activity of amphiphilic block co-polymers, these mixtures (dissolved in DCM as the oil phase) were emulsifed in water with a water:oil ratio of 5:1. Nile Red was dissolved in the oil phase as an indicator. Pristine hydrophobic PS-*b*-P4VP was tested as the control, and as expected, clear segregation of water and oil emerged immediately after emulsification (**Figure 2**a). With a little change in amphiphilicity, an obvious W/O emulsion—that is, Emulsion 1–0.05 (referring to the emulsion stabilized by Mixture 1-0.05) was formed (Figure 2d,i). According to the Bancroft rule, this is because the quite hydrophobic skeleton favors forming W/O emulsions.[11] In contrast, using a largely enhanced amphiphilic mixture, catastrophic phase inversion occurred, resulting in an O/W emulsion (Emulsion 1–0.5; Figure 2g,l) and a W/O/W double emulsion (Emulsion 1–1; Figure 2h,m), similar to our previous work using homogenization.[10] Surprisingly, a W/O HIPE was obtained when the amphiphilicity degree of the polymer was enhanced, but not to the extent that would be strong enough for phase inversion. Microscopic polyhedral structures as well as polydisperse sizes are clearly illustrated in Emulsion 1–0.2 (Figure 2e,j) and Emulsion 1–0.3 (Figure 2f,k). Figure 2b displays the evident concave hole in the "gel" emulsion after emulsification; this is a direct demonstration of the production of thixotropic non-Newtonian fluids.[1a] In contrast to Emulsion 1–0.3, which revealed a certain flow behavior after several minutes (Figure S1, SI), the Emulsion 1–0.2 possessed a more extraordinary gel-like property that slid little even if the vial was placed upside down for two weeks (Figure 2c).

In view of the optimal amphiphilicity for HIPE preparation provided by Mixture 1–0.2 at a concentration of 20 mg mL^{-1} with respect to the DCM, we further varied the water:oil ratio based on this mixture to investigate

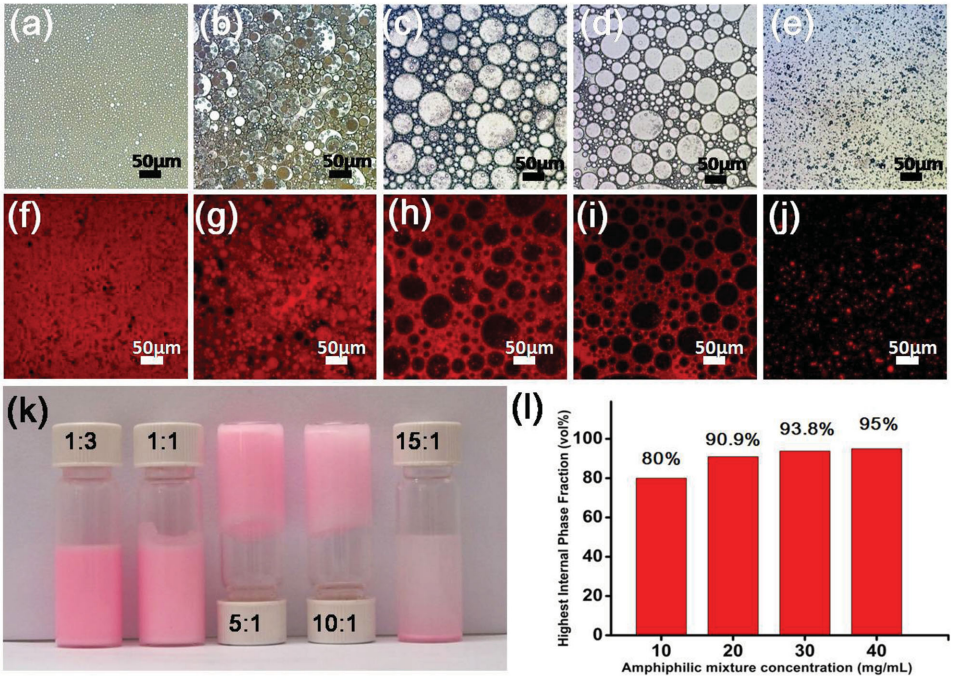

Figure 3. a–e) Bright-field microscopy, f–j) fluorescence microscopy, and k) optical images of the emulsions prepared using the amphiphilic Mixture 1–0.2 with a water:oil ratio of 1:3 (a,f), 1:1 (b,g), 5:1 (c, h), 10:1 (d, i), and 15:1(e, j). l) The highest internal-phase volume fraction of the HIPEs using the amphiphilic Mixture 1–0.2 while varying the concentration.

phase-inversion behavior. According to the Bancroft rule, the phase where the emulsifier preferentially dissolves is always viewed as the continuous phase.[11] Because the amphiphilic mixture is dissolved in DCM, a typical W/O emulsion with the water:oil ratio of 1:3 is clearly shown in **Figure 3**a and f. When the water volume was raised to 50%, O/W emulsion droplets inside the W/O emulsion appeared, as a consequence of catastrophic phase inversion (Figure 3b,g); however, instead of a complete phase inversion, a W/O HIPE with a water:oil ratio of 5:1 was obtained (Figure 3c,h). The highest internal-phase volume fraction in this mixture concentration was 90.9%, a significantly high internal-phase fraction at a low concentration compared to what can be obtained with conventional surfactants or particle stabilizers. At a water:oil ratio of 15:1, we could only obtain a phase-inversion-induced O/W emulsion due to the inadequate content of the amphiphilic mixture (Figure 3e,j). To elucidate this observation, the concentration of the amphiphilic mixture was increased to 40 mg mL^{-1}, at which a highest internal-phase volume of 95% was achieved (Figure 3i). Furthermore, conductivity measurements were used to compare the polymer amphiphilicity as well as characterize the emulsion type, where the O/W emulsion and W/O/W double emulsion typically exhibit a higher conductivity of more than 200 μS cm^{-1} (Figure S2, SI).

The formation of W/O HIPE principally relies on the stable amphiphilic structure caused by the quaternization of the P4VP segment. CF_3COOH in this work is chosen to be the amphiphilicity "adjuster" of PS-*b*-P4VP because it is a considerably strong organic protonic acid (pK_a = 0.23). As a consequence, it more inclined to donate its proton to the electron-rich pyridine groups, eventually leading to more robust electrostatic combinations. As a control, we also tested CH_3COOH (pK_a = 4.76) as an "adjuster" to the PS-*b*-P4VP amphiphilicity. Although the polymer became amphiphilic to some extent, only W/O emulsions could be obtained using polymer-CH_3COOH mixtures with pyridine:carboxyl ratios of 1:0.2, 1:0.5 and 1:1 (Figure S3, SI). In addition, the emulsification method also makes a great difference. Because HIPEs are a type of Bingham fluids, which suffer collapse beyond critical shear stress, a gentle vortex emulsification is required.[1a] Vigorous high-speed homogenization, as we previously used,[10] and ultrasonic emulsification will give rise to various emulsions but not to any HIPEs.

2.3. HIPE-Templated Macroporous Monoliths (HMMs)

To verify the applicability of these HIPEs to serve as templates for macroporous structures, photopolymerization using the photocurable monomer, triacrylate (Chart S1, SI), and the photoinitiator HCPK (hydroxycyclohexyl phenyl ketone) is pursued to construct a polymer scaffold. Triacrylate is an oil-soluble monomer with three vinyl end groups, which can be polymerized into a polymer network, and an extra cross-linker is not necessary. Rapid photopolymerization, which requires only a few minutes, can effectively "fix" the HIPE template prior to destabilization of the emulsion, making such polymerization more suitable for our system than thermally initiated polymerization.[12] The characteristic morphologies of well-defined 3D HIPE-templated macroporous monoliths including closed and open cells are demonstrated in **Figure 4** (also see SI: Table S2); the HMM's are abbreviated as HMM 1, HMM 2, HMM 3, HMM 4, and HMM 5. The open-cell macroporous structure refers to macropores (or void pores)

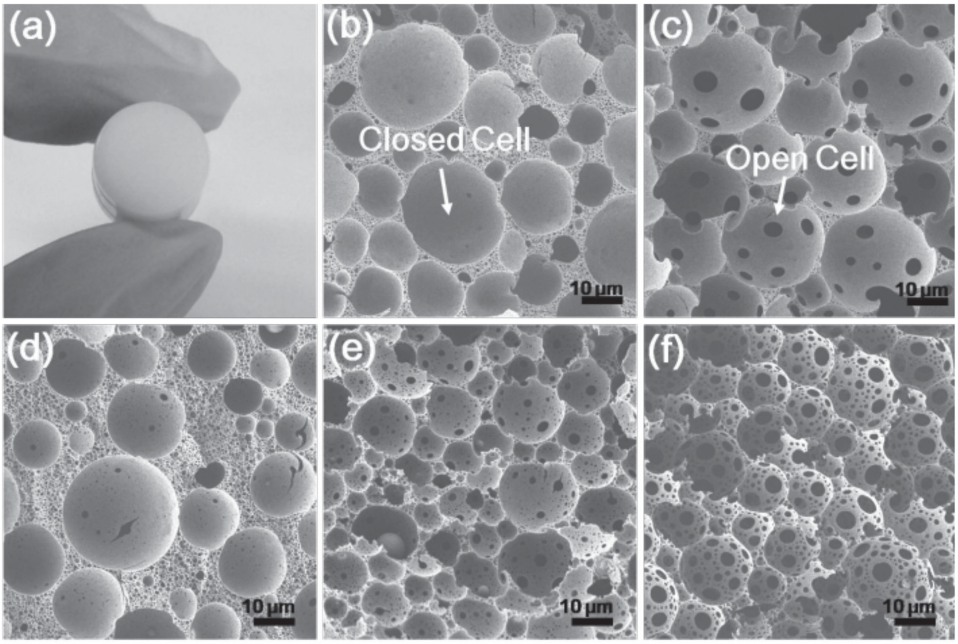

Figure 4. a) Optical image of the HIPE-templated macroporous monolith (HMM). b–f) Scanning electron microscopy (SEM) images of the HMM using Mixture 1–0.2 with a water:oil ratio of 3:1 (b, HMM 1) and 5:1 (c, HMM 2) at a concentration of 20 mg mL^{-1} with respect to the DCM, and with the water:oil ratio of 3:1 (d, HMM 3), 5:1 (e, HMM 4), and 10:1 (f, HMM 5) at a concentration of 40 mg mL^{-1}.

with a diameter of ≈5–50 μm, which are interconnected with "window" or "throat" pores with a size of ≈1–5 μm. Many examples show that the polymerization of HIPEs stabilized by molecular surfactants normally results in open-cell pores. One main reason for this is that when a large amount of surfactant is required (above 5 wt%), there is an obvious inclination towards open cells.[2b,13] Due to the merit of reduced amounts of surfactant, closed-cell pores can also exist in our system when the internal phase is not very high. Because the formation of throat pores is a result of the shrinkage of the contact domain after the curing process, the internal-phase volume and the surfactant content—the tools that thin the contact domain—play important roles in the openness of the macropores. Our results reveal that these throat pores mainly arise from the higher internal-phase volume. At the amphiphilic mixture concentration of 20 mg mL^{-1} (with respect to DCM), it is apparent that the HIPE with an 83.3% internal phase forms open cells (HMM 1); meanwhile the HIPE with a 75% internal phase produces closed cells (HMM 2, Figure 4b,c). This viewpoint is further evidenced by the use of a higher mixture concentration (40 mg mL^{-1}), in which a highly interconnected macroporous structure is clearly observed with the water:oil ratios of 5:1 (Figure 4e, HMM 4) and 10: 1 (Figure 4f, HMM 5). The enhanced concentration of the amphiphilic mixture also increases the quantity of the "throat" pores, but relatively speaking, it is not as obvious as the internal phase volume fraction.

2.4. PPy-Coated HMM and Filtration of Bacteria

In light of the interconnected macroporous structure, we envision the open-cell HMM to be exploited as a novel bacteria filter responsive to the near infrared (NIR). In this tentative application, the HMM would be able to exclude oversized bacteria similar to conventional filters, and meanwhile inactivate the bacteria using a NIR-induced high-temperature environment. NIR can be a remotely controlled stimulus, possessing numerous advantages over some other reported triggers such electric fields and UV light; for example, it is less hazardous to the human body, and it exhibits a highly penetrating power and precise positioning.[14] In order to enhance the photothermal conversion efficiency, polypyrrole (PPy) nanoparticles, a typical NIR-responsive "nanoheater", were introduced into the HMM via a post-polymerization process. After successfully coating the HMM with PPy particles, the surface of the macropores became rougher, which helped filtration (**Figure 5**a). More importantly, rapid heating of the PPy-coated HMM from 20 to around 180 °C was observed from the thermal images within 10 s, while the control HMM remained around 20 °C under the same conditions (Figure 5b; Figure S4, SI).

As a proof-of-concept study, a common gram-negative bacterial suspension, *Escherichia coli* (*E. coli*, ATCC 25922), was pumped to flow through the samples. Turbidity measurements give a lower optical density value for the PPy-coated HMM after the filtration (Figure 5c), indicating that the filtration ability of the PPy-coated HMM is higher than that of the control HMM. Furthermore, the bacteria that failed to be excluded by the macropores were killed during the filtration by the NIR light illumination (808 nm, 1.11 W cm^{-2}). Based on the standard plate-count method, colony counting of the filtered suspension showed an antibacterial efficiency of 42% for the control HMM at a flow rate of 25 μL min^{-1}. In contrast, with the PPy coating, the antibacterial efficiencies of the HMMs increased with a decrease in flow rate, reaching a

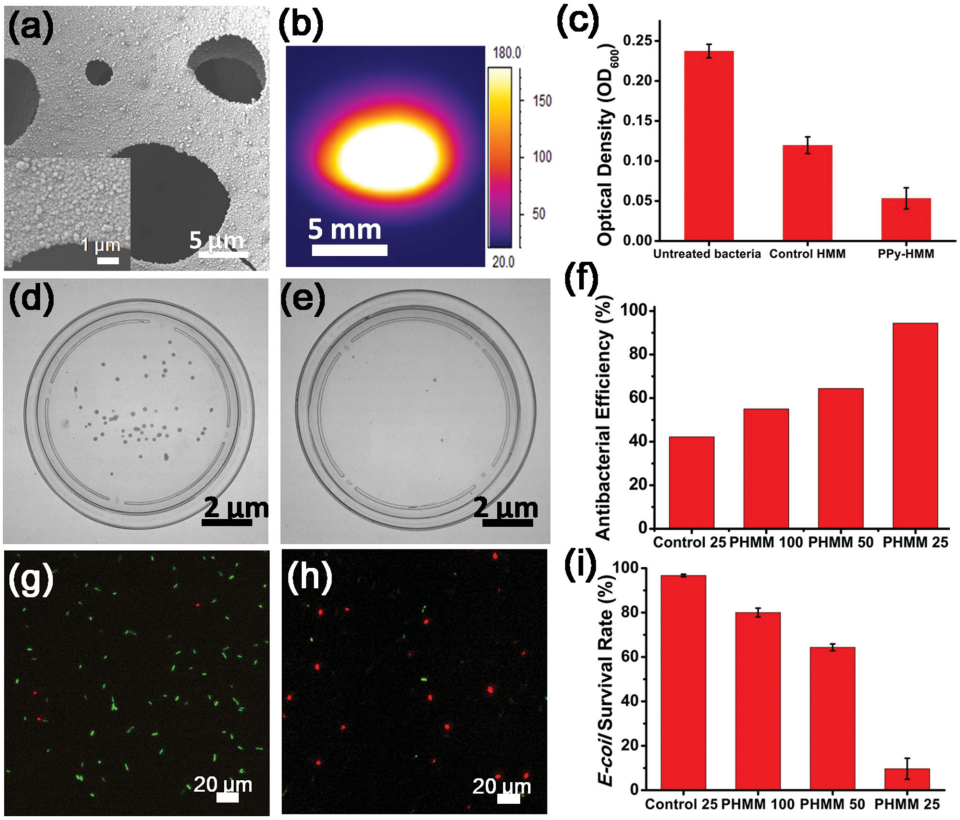

Figure 5. a) SEM images of the open-cell PPy-coated HMM. b) Thermal image of the photothermal conversion of PPy-coated HMM after irradiation with a NIR source (808 nm, 1.11 W cm^{-2}) for 10 s. The color scale indicates the temperature in °C. c) Optical density (OD_{600}, at the wavelength of 600 nm) values of the *E. coli* suspensions before and after filtration through the control HMM and the PPy-coated HMM. d,e) Plate photographs and g,h) fluorescence microscopy images of the *E. coli* suspensions after filteration through the control HMM (d,g) and the PPy-coated HMM (e,h) under NIR irradiation at a flow rate of 25 μL min^{-1}. f,i) The calculated antibacterial efficiency based on colony counting (f) and bacterial survival rate calculated based on the LIVE/DEAD assay (i) at a flow rate of 100, 50, and 25 μL min^{-1} (designated as PHMM 100, PHMM 50, and PHMM 25, respectively). The control measurements in (f,i) had a flow rate of 25 μL min^{-1}.

maximum efficiency of 94% at the aforementioned flow rate (Figure 5d–f; Figure S5, SI). As a result, the enhanced efficiency was ascribed to the photothermal conversion of the PPy nanoparticles, which produced adequate heat capable of killing the bacteria. The LIVE/DEAD assay was performed to verify this hypothesis. The unfiltered *E. coli* bacteria were stained with fluorochromes STYO-9/PI to label the living and dead bacteria with green and red fluorescence, respectively. As illustrated in Figure 5g–i, about 95% of the bacteria flowing through the PPy-coated HMM was inactivated at a flow rate of 25 μL min^{-1}, while the control HMM system barely produced any dead bacteria under the same conditions. Combining the abilities of both bacteria filtration and inactivation, these results suggest that this PPy-coated HMM is a promising candidate for water sterilization.

3. Conclusion

In summary, we have demonstrated that through progressively tailoring the amphiphilicity using trifluoroacetic acid, the originally hydrophobic block co-polymer PS-*b*-P4VP is capable of being a surfactant for HIPEs. The required concentration of the polymer in this approach is below 5 wt%, and the resulting HIPEs can reach a considerably high internal-phase volume of 95%. W/O HIPEs tend to form at an amphiphilic degree between that of normal W/O emulsions and that of phase-inversion-induced O/W or W/O/W abnormal emulsions. The selection of the amphiphilicity "adjuster" plays a significant role in designing an suitable amphiphilic structure for the HIPE preparation. Due to the low amounts of surfactant required in our system, well-defined, closed- and open-cell 3D macroporous architectures are both fabricated based on these HIPE templates. We finally demonstrate that the resulting highly interconnected macroporous monoliths can be exploited as novel NIR-sensitive bacteria filters. We believe this work will encourage a much wider utilization of the block co-polymers as HIPE surfactants, opening avenues for significant diversity in functional macroporous materials.

4. Experimental Section

Preparation of the Amphiphilic Mixtures and Amphiphilicity Characterization: A simple route was used to prepare the polymer–(organic acid) mixtures with different amphiphilicity. Typically, 4.34 μL of CF_3COOH was mixed into 4 mL of DCM as the amphiphilicity "adjuster" mother solution. For 0.5 mL of a PS-*b*-P4VP

solution (20 mg mL^{-1} in DCM), 5, 20, 30, 50, and 100 μL of the CF_3COOH mother solution was added to obtain amphiphilic mixtures with the molar ratios of 1:0.05, 1:0.2, 1:0.3, 1:0.5, 1:1 for the pyridine groups to the carboxyl groups.

The water contact angles of different amphiphilic blends were measured and captured on an optical contact-angle measuring device (OCA 20, Dataphysics Instruments GmbH). Before that, the amphiphilic mixture solutions were spin-coated on glass substrates and dried at 45 °C to form robust and uniform films. The surface energies were calculated according to the classic Owens–Wendt–Kaelble (OWK) method. Generally, two standard probe liquids, whose surface energy (γ_L) and its dispersive (γ^d_L) and polar component (γ^P_L) are known, were dropped on the spin-coated film for contact angle measurements. The probe liquids used here were pure water (H_2O) and diiodomethane (CH_2I_2). Afterwards, we acquired two binary equations and then determined the dispersive (γ^d_S) and the polar components (γ^P_S) of the surface energy of the polymer based on the OWK equation; that is,

$$\gamma_L(1+\cos\theta) = 2\sqrt{\gamma_S^d\gamma_L^d} + 2\sqrt{\gamma_S^p\gamma_L^p} \quad (1)$$

Then the polymer surface energy is

$$\gamma_S = \gamma_S^d + \gamma_S^p \quad (2)$$

The FTIR spectra to characterize hydrogen-bond interactions between the pyridine groups and carboxyl groups were obtained using a Bruker Tensor 27.

Preparation and Characterization of HIPEs and HMMs: For the emulsion preparation, the oil phase consisted of the aforementioned amphiphilic mixtures, and the water was distilled water. Water and oil phases were mixed at a water:oil ratio of 5:1 and then emulsified on a vortex (IKA MS 3) with a rotation speed of 1300 rpm for 15 min. Various emulsions, including W/O emulsions, W/O HIPE emulsions, O/W emulsions, and W/O/W double emulsions, were obtained by using different amphiphilic mixtures. The influence of the water:oil ratio and amphiphilic mixture concentration were also determined using a similar process.

For HMM preparation, 0.2 mL of the photopolymerizable solution comprising the triacrylate monomer and 0.5 wt% photoinitiator HCPK was prepared and then added to 0.5 mL of the oil phase containing Mixture 1–0.2. The emulsification process followed the same process as discussed above. Then the prepared HIPEs were subjected to UV irradiation (16.8 mW cm^{-2}) for 7 min for the first photopolymerization. The HMMs were then placed upside down for a second irradiation to ensure adequate polymerization. Finally, the obtained HMMs were washed several times in ethanol in order to remove any unpolymerized monomer.

A commercial digital camera (Olympus, E-PM1) was employed to acquire macroscopic pictures of the emulsions. The bright-field images of the emulsions and particles in aqueous state were provided by a fluorescent optical microscope (Scope A1, Axio Zeiss). The images of the HMMs after being dried in the air were captured by a scanning electron microscope (JEOL 6700); spurting a layer of gold membrane over the surface of the materials was necessary prior to imaging. The porosity of the macroporous architecture was measured by mercury intrusion porosimetry (Demo Autopore IV 9500). The skeletal density (SD) of the materials was calculated based on the solid monolith containing polymerized triacrylate and (PS-*b*-P4VP)–CF_3COOH mixture using the Archimedes methods. Typically, we measured the mass of the solid monolith in air (m_1). Then, after being tied to a thin rope, the monolith was suspended in the middle of a beaker of water. The mass before (m_2) and after (m_3) the monolith was suspended in water was recorded. The skeletal density is thus SD = $m_1/(m_3-m_2)$.

Preparation of the PPy-Coated HMM and Filtration of the Bacterial Suspension: For the bacteria filtration, the selected HMM originated from the HIPE with a water:oil ratio of 5:1 and the amphiphilic Mixture 1–0.2 at a concentration of 40 mg mL^{-1} because this HMM has a high interconnected structure with the appropriate size for capturing bacteria. PPy-coated HMM was fabricated via post-polymerization of the polypyrrole (PPy) nanoparticles. Generally, the HMM was fully soaked in a monomer solution containing pyrrole monomer and ethanol (pyrrole: ethanol = 1:10). After removing the superfluous monomer solution, the sample was transferred to a ferric chloride solution (92 mg mL^{-1}) and stocked in 4 °C for the PPy polymerization. This process was repeated twice in order to ensure a full coating of PPy nanoparticles onto the HMM. At last, the PPy-coated HMM was washed with ethanol 5× and dried in air for the bacteria filtration. A continuous NIR laser (808 nm, HTOE, Beijing) was triggered to illuminate the HMMs and a thermal IR imager (IR-384, RNO) was used to record the temperature change in situ.

E. coli bacteria were cultured in Luria–Bertani broth medium (LB, Sigma-Aldrich) in the incubator shaker at 37 °C at a speed of 200 rpm for 12 h and used as the stock suspension. The concentration of bacteria could be monitored by measuring the optical density (OD) at a wavelength of 600 nm (Shanghai Metash Instrument Co. Ltd.). Before the filtration, the bacterial suspension was harvested by centrifugation and washing with phosphate buffer solution (PBS). It was adjusted to the OD value of around 0.25.

A certain amount of bacterial suspension was transferred to a syringe, which was then fixed on a syringe pump. The control HMM and PPy-coated HMM were immobilized on the syringe tip. The filtration was performed driven by the pump at flow rates of 100, 50, and 25 μL min^{-1}. During the filtration, the HMMs were subjected to NIR irradiation at a power density of 1.11 W cm^{-2}. The resulting bacterial suspension was collected for further analysis.

Plate Counting Method and LIVE/DEAD Assay: The resulting bacterial suspension was serially diluted (1.25×10^4 times) in PBS solution. Then 5 μL of suspension was spread on the solid LB agar. After incubation at 35 °C for 24 h, colonies formed. The number of the colonies was counted. The antibacterial effciencies were calculated based on these colony countings, in which the originally untreated bacterial suspension was regarded as 100%.

The LIVE/DEAD bacterial assay was applied to rapidly estimate the bacterial vitality after filtration. Briefly, the resulting bacterial suspension was centrifuged and re-adjusted to 0.5 mL. Afterwards, 2.5 μL of STYO-9 dye (5 mol mL^{-1}) and 5 μL of propidium iodide dye (PI, 5 mol mL^{-1}) were added to the bacterial suspension and kept for 20 min. The green-fluorescence SYTO-9 dye could enter both intact and membrane-compromised bacterial cells, while the red-fluorescence PI dye only entered membrane-damaged cells and covered up the green fluorescence. Consequently, the live and dead bacteria would display green and red fluorescence, respectively, under the inverted fluorescence microscope (Eclipse Ti, Nikon, Japan). The bacterial survival rates were calculated by analyzing the fluorescent images.

Supporting Information

Supporting Information is available from the Wiley Online Library or from the author. It includes the characterization of the plate-counting graphs, conductivity measurements, contact angles measurements, and calculation of surface energies.

Acknowledgements

X.H. and Y.Y. contributed equally to this work. Financial support was provided by the National Natural Science Foundation of China (51373197, 21422407), Program for New Century Excellent Talents in University (NCET-12–0530).

[1] a) H. Zhang, A. I. Cooper, *Soft Matter* **2005**, *1*, 107–113; b) M. S. Silverstein, N. R. Cameron, in *Encyclopedia of Polymer Science and Technology*, John Wiley & Sons, New York, NY **2010**, DOI: 10.1002/0471440264.pst571; c) N. R. Cameron, D. C. Sherrington, *Adv. Polym. Sci.* **1996**, *126*, 163–214; d) M. S. Silverstein, *Prog. Polym. Sci.* **2014**, *39*, 199–234.

[2] a) S. D. Kimmins, N. R. Cameron, *Adv. Funct. Mater.* **2011**, *21*, 211–225; b) N. R. Cameron, *Polymer* **2005**, *46*, 1439–1449; c) A. Imhof, D. J. Pine, *Nature* **1997**, *389*, 948–951; d) J. Ma, Y. S. Hui, M. Zhang, Y. Yu, W. Wen, J. Qin, *Small* **2013**, *9*, 497–503.

[3] a) Y. Xia, B. Gates, Y. Yin, Y. Lu, *Adv. Mater.* **2000**, *12*, 693–713; b) C. Liang, Z. Li, S. Dai, *Angew. Chem. Int. Ed.* **2008**, *47*, 3696–3717; c) Z. Niu, L. Liu, L. Zhang, X. Chen, *Small* **2014**, *10*, 3434–3441.

[4] a) A. I. Cooper, *Adv. Mater.* **2003**, *15*, 1049–1059; b) Q. Li, L. M. Matuana, *J. Appl. Polym. Sci.* **2003**, *88*, 3139–3150; c) R. Butler, I. Hopkinson, A. I. Cooper, *J. Am. Chem. Soc.* **2003**, *125*, 14473–14481.

[5] a) J. M. Williams, *Langmuir* **1991**, *7*, 1370–1377; b) K. Haibach, A. Menner, R. Powell, A. Bismarck, *Polymer* **2006**, *47*, 4513–4519; c) A. Barbetta, N. R. Cameron, *Macromolecules* **2004**, *37*, 3188–3201.

[6] a) P. A. Kralchevsky, I. B. Ivanov, K. P. Ananthapadmanabhan, A. Lips, *Langmuir* **2005**, *21*, 50–63; b) B. P. Binks, S. O. Lumdson, *Langmuir* **2000**, *16*, 2539–2547; c) P. J. Colver, S. A. F. Bon, *Chem. Mater.* **2007**, *19*, 1537–1539.

[7] a) V. O. Ikem, A. Menner, A. Bismarck, *Angew. Chem. Int. Ed.* **2008**, *47*, 8277–8279; b) S. G. Zhang, J. D. Chen, *Chem. Commun.* **2009**, *16*, 2217–2219; c) Z. F. Li, T. Ming, J. F. Wang, T. Ngai, *Angew. Chem. Int. Ed.* **2009**, *48*, 8490–8493; d) G. Sun, Z. Li, T. Ngai, *Angew. Chem. Int. Ed.* **2010**, *49*, 2163–2166; e) V. O. Ikem, A. Menner, T. S. Horozov, A. Bismarck, *Adv. Mater.* **2010**, *22*, 3588–3592.

[8] a) A. May, K. Aramaki, J. M. Gutierrez, *Langmuir* **2011**, *27*, 2286–2298; b) J. Li, J. Zhang, Y. Zhao, B. Han, G. Yang, *Chem. Commun.* **2012**, *48*, 994–996; c) A. Menner, R. Powell, A. Bismarck, *Soft Matter* **2006**, *2*, 337–342; d) S. Kovacic, N. B. Matsko, K. Jerabek, P. Krajnc, C. Slugovc, *J. Mater. Chem. A* **2013**, *1*, 487–490; e) N. R. Cameron, D. C. Sherrington, *Macromolecules* **1997**, *30*, 5860–5869.

[9] a) P. Viswanathan, S. Chirasatitsin, K. Ngamkham, A. J. Engler, G. Battaglia, *J. Am. Chem. Soc.* **2012**, *134*, 20103–20109; b) P. Viswanathan, D. W. Johnson, C. Hurley, N. R. Cameron, G. Battaglia, *Macromolecules* **2014**, *47*, 7091–7098.

[10] a) X. Huang, Q. Qian, Y. Wang, *Small* **2014**, *10*, 1412–1420; b) D. Wang, X. Huang, Y. Wang, *Langmuir* **2014**, *30*, 14460–14468; c) X. Huang, R. Fang, D. Wang, J. Wang, H. Xu, Y. Wang, X. Zhang, *Small* **2015**, *11*, 1537–1541; d) J. Wang, J. Zhao, Y. Li, M. Yang, Y.-Q. Chang, J.-P. Zhang, Z. Sun, Y. Wang, *ACS Macro Lett.* **2015**, *4*, 392–397.

[11] a) M. F. Ficheux, L. Bonakdar, F. Leal-Calderon, J. Bibette, *Langmuir* **1998**, *14*, 2702–2706; b) J. M. Morais, O. D. Santos, J. R. Nunes, C. F. Zanatta, P. A. Rocha-Filho, *J. Dispersion Sci. Technol.* **2008**, *29*, 63–69; c) J. M. Morais, P. A. Rocha-Filho, D. J. Burgess, *Langmuir* **2010**, *26*, 17874–1788.

[12] a) S. D. Kimmins, P. Wyman, N. R. Cameron, *React. Funct. Polym.* **2012**, *72*, 947–954; b) X. Zhang, D. Ji, T. Lei, B. Zhao, K. Song, W. Hu, J. Wang, J. Pei, Y. Wang, *J. Mater. Chem. A* **2013**, *1*, 10607–10611.

[13] J. M. Williams, D. A. Wrobleski, *Langmuir* **1988**, *4*, 656–662.

[14] a) X. Huang, Q. Qian, X. Zhang, W. Du, H. Xu, Y. Wang, *Part. Part. Syst. Charact.* **2013**, *30*, 235–240; b) Q. Qian, X. Huang, X. Zhang, Z. Xie, Y. Wang, *Angew. Chem. Int. Ed.* **2013**, *52*, 10625–10629; c) H. Jia, J. Wang, X. Zhang, Y. Wang, *ACS Macro Lett.* **2014**, *3*, 86–90; d) L. C. Kennedy, L. R. Bickford, N. A. Lewinski, A. J. Coughlin, Y. Hu, E. S. Day, J. L. West, R. A. Drezek, *Small* **2011**, *7*, 169–183; e) D. T. Schoen, A. P. Schoen, L. Hu, H. S. Kim, S. C. Heilshorn, Y. Cui, *Nano Lett.* **2010**, *10*, 3628–3632; f) K. Liu, Y. Liu, Y. Yao, H. Yuan, S. Wang, Z. Wang, X. Zhang, *Angew. Chem. Int. Ed.* **2013**, *52*, 8285–8289.

Received: May 17, 2015
Published online: June 25, 2015

